

**R. K. KHALKECHEV**<sup>1</sup>, Professor, Doctor of Engineering Sciences, Associate Professor, syrus@list.ru  
**E. A. KALASHNIKOV**<sup>1</sup>, University of Science and Technology—NUST MISIS, Associate Professor, Candidate of Engineering Sciences  
**S. V. SOLODOV**<sup>1</sup>, Head of Institute, Candidate of Engineering Sciences, Associate Professor

<sup>1</sup>National University of Science and Technology—NUST MISIS, Moscow, Russia

## AUTOMATED SYSTEM FOR ANALYZING STABILITY OF PITWALL SLOPE AREAS PRONE TO ROTATIONAL LANDSLIDES

### Introduction

Mineral mining at deeper levels and the increased demand to reduce expenses of production in the mining sector leads to planning higher steep slopes in open pit mines [1]. As a consequence, the number of slope instability events in the form of various landslides currently grows. Practice shows that such events can cause injuries and failure of mining machines and equipment [2].

Solving of this problem commonly involves various program products for the slope stability analysis in open pit mines to discern a landslide and to prevent its risk. Currently, many methods are included in the program products of the slope stability analysis [1]: kinematic [3, 4]; limit equilibrium [5, 6]; finite differences [7, 8]; finite elements [9, 10]; discrete elements [11–13], etc.

The programming support practice in industry shows that among the above-listed methods of the slope stability analysis, the highest accuracy of landslide modeling is a feature of the methods of discrete differences, finite elements and discrete elements. However, despite all advantages, these methods have two basic demerits. The first lies in the process of selecting a correct procedure for discretization of a space of a problem solution, namely, in all studies in this field of research, discretization procedures disregard a representative volume of rocks, i.e. the volume where rocks start displaying their macroscopic physical properties [14]. This certainly worsens the instability prediction accuracy.

The second shortage is that the slope stability analysis of pitwall hazardous in terms of rotational slides assumes that formation of a surface of rotation immediately induces instability and landslide descent. This is a misthought which is many times disproved practically: the main body of landslide, that is formed or nearly formed, can for a long time exist in the condition of small displacements along the slope, without posing threat to mining operations.

Considering the above stated, the main objective of the research is development of a new automated slope stability analysis system for open pits with regard to the representative volume of rocks and the real mechanism of rotational slides.

### Materials and methods

For developing the proposed system, a new algorithm is proposed for the slope stability analysis in open pits with regard to fulfillment of rotational slides. Let us set the main requirements for the algorithm.

Let a potential body of slide be a site of pitwall composed of rocks with different physical properties. As observations show, there are two types of instability of a potential slide body—local and global. The local instability is conditioned by rotation of a potential body of slide, leading to slight displacements of rocks along the lower bench of pitwall, which bring no considerable hazard to mining operations. The global instability represents rotation of a potential slide body as a whole entity with the subsequent failure and landslide descent.

*The presented article proposes an automated system for analyzing potentially dangerous sites of pitwall slopes in terms of rotational landslides. An algorithm is developed to implement the automated system software, which enables analysis of potential landslide bodies with regard to nonuniform distributions of rock densities and displacements caused by rainfall. The algorithm application allows identifying two types of instability of pitwall slopes—local and global. The local instability results from rotation of a potential landslide body, leading to minor rock displacements toward the lower bench of the pit. This type of instability poses no significant danger to mining operations. The global instability is characterized by rotation of a landslide body as a whole, followed by subsequent destruction and collapse of rock mass toward the lower bench. The automated system software architecture comprises three subsystems. The first subsystem collects data on rock moisture, density and displacements on a test pitwall slope site using geodetic equipment, moisture sensors and laboratory density tests. The second subsystem analyzes these data to detect the local and global instability. Finally, the third subsystem processes and stores all relevant datasets on rock densities, displacements and moisture content for the studied area. To verify the adequacy of the obtained solutions, the proposed system was tested at the Dzhegonas Quarry in the Karachay-Cherkess Republic of the Russian Federation. The results showed that for the proposed system, the performance metric—percentage of correct decisions in the analysis of slope stability in terms of rotational landslide occurrence—was 90%. Meanwhile, for the software tools previously used at the quarry, this figure was 60%.*

**Keywords:** potential landslide body, local instability, global instability, algorithm, nonuniform density field, nonuniform displacement field, spatial discretization

**DOI:** 10.17580/em.2026.01.09

Thus, the first requirement for the algorithm is to detect the local and (or) global instability on the pitwall slope sites.

For building the algorithm, we use the model from the study [15]. According to this model, a potential body of slide is affected by the resultant vertical force applied to the gravitational center  $C$  of the buried part of the slide body, as well as the cohesion force which restrains the body. The equilibrium condition of these forces depends on the position (in other words, configuration) of the buried part of a potential slide body, set in terms of an angle  $\varphi$  relative to the vertical axis, and in terms of the gravitational center  $C$  (coordinates of the latter depend on  $\varphi$ , too). As a result, the local equilibrium of a potential slide body can be described by the value of  $C(\varphi)$ . The model finds out that the local instability shows up at the fulfillment of a rotary moment connected with the position  $C(\varphi)$  and the gravity  $T$  of the whole body. Unfortunately, the model lacks a formalized approach to determining  $C(\varphi)$ . The reasons are: (1) it is unknown how to delineate the buried part of a potential slide body; (2) a potential slide body is analyzed as a two-dimensional feature; (3) the problem neglects a key factor of landsliding—rain precipitations [16, 17]. In this manner, we arrive at a final and basic requirement—the algorithm is to determine the value of  $C(\varphi)$  with the delineation of a three-dimensional buried part of a potential slide body in the conditions of rain precipitation.

The above-listed requirements allow creating the following generalized algorithm for the stability estimation of pit slopes in case of a rotational slide. In this connection, we use the notation offered by Knuth [18]. So, the steps of the algorithm are described below.

1. *Detecting a potential body of slide.* The boundary of a potential slide body as a three-dimensional feature is determined on pitwall slope using surveying instruments.

2. *Building an empty 3D block model.* The delineated three-dimensional potential body of slide is split into a set of regular cubic blocks. The size of a block is to be set as the largest representative volume  $V$  of rocks inside the potential body of slide. To this effect, it is possible to use the method from the study [19]. As a result, we compose a 3D body  $b[N_x, N_y, N_z]$ , where  $N_x, N_y, N_z$  is the number of blocks along the axis  $O_x, O_y$  and  $O_z$ , respectively.

3. *Building a 3D reference block model  $L$  of a potential body of slide.* Using certain experimental techniques and equipment, the values of the displacement vector  $u = (n_x, n_y, n_z)$ , the density  $\rho_d$  of dry rocks and their moisture content  $w$  are obtained at the uniformly spaced points of the potential body of slide, conformable with certain blocks. The values in the rest blocks are determined by one of the most suitable method of kriging [20]. As a result, a 3D reference block model of a potential slide body is obtained:  $L = \{b[N_x, N_y, N_z], u[N_x, N_y, N_z], \rho d[N_x, N_y, N_z], w[N_x, N_y, N_z]\}$ , where  $u[N_x, N_y, N_z]$  is the 3D array of displacements;  $\rho d[N_x, N_y, N_z]$  is the 3D array of densities of dry rocks;  $w[N_x, N_y, N_z]$  is the 3D array of moisture contents of rocks.

4. *Delineating a buried part of a potential body of slide.* By analyzing the values of the displacement vector, the blocks  $b[i, j, k]$  with the positive displacements (which points at the displacement in the direction of the slope) are identified. The set of these blocks is the buried part of the potential slide body. The model is added with an attribute of the membership of the buried part:  $L = \{b[N_x, N_y, N_z], u[N_x, N_y, N_z], \rho d[N_x, N_y, N_z], w[N_x, N_y, N_z], q[N_x, N_y, N_z]\}$ , where  $q[i, j, k] = 1$  at  $i = 1 \dots N_x, j = 1 \dots N_y, k = 1 \dots N_z$  if a block belongs in the buried part and  $q[i, j, k] = 0$  in the opposite case.

5. *Building a 3D block model  $M$  of a potential body of slide with regard to rain precipitations.* The densities of moist rocks is determined in each block from the expression  $\rho[i, j, k] = \rho d[i, j, k](1 + w[i, j, k])$  at  $i = 1 \dots N_x, j = 1 \dots N_y, k = 1 \dots N_z$ . The result is a 3D block model of a potential slide body with regard to rain precipitations:  $M = L = \{b[N_x, N_y, N_z], u[N_x, N_y, N_z], \rho[N_x, N_y, N_z], q[N_x, N_y, N_z]\}$ , where  $\rho[N_x, N_y, N_z]$  is the density of moist rocks.

6. *Building a set of 2D block models  $M = \bigcup_{i_0=1}^{N_x} M[i_0]$  of a potential body of slide with regard to rain precipitations.* The 3D model is divided into a set of 2D models (sections) along the axis  $Ox$  (with recording the index  $i$ ):  $M = \bigcup_{i_0=1}^{N_x} M[i_0]$ , where  $M[i_0] = \{b[i_0, j, k], u[i_0, j, k], \rho[i_0, j, k], q[i_0, j, k]\}$  at  $j = 1 \dots N_y, k = 1 \dots N_z$ .

7. Attributing value 1 to the index  $i_0$  pointing at 2D block model being analyzed:  $i_0 \leftarrow 1$ .

8. For the 2D block model  $M[i_0]$ , the gravity  $T[i_0]$  of a section as a whole entity is determined as  $T[i_0] = (y_T[i_0], z_T[i_0])$  using the following formulas:

$$y_T[i_0] = \frac{\sum_{j=1}^{N_y} \sum_{k=1}^{N_z} y[i_0, j, k] \cdot m[i_0, j, k]}{\sum_{j=1}^{N_y} \sum_{k=1}^{N_z} m[i_0, j, k]}$$

$$z_T[i_0] = \frac{\sum_{j=1}^{N_y} \sum_{k=1}^{N_z} z[i_0, j, k] \cdot m[i_0, j, k]}{\sum_{j=1}^{N_y} \sum_{k=1}^{N_z} m[i_0, j, k]}$$

where  $(y[i_0, j, k], z[i_0, j, k])$  are the coordinates of a block center in the 2D model;  $m[i_0, j, k] = \rho[i_0, j, k]V$  is the mass of a block in the 2D model.

9. For the 2D block model  $M[i_0]$ , the gravitational center  $C[i_0]$  of a section of the buried part of a slide body is determined. For the blocks with  $q[i_0, j, k] = 1$ , the gravitational center  $C[i_0] = (y_C[i_0], z_C[i_0])$  is determined for  $\varphi_0$  (the current position of a section of the buried part of a potential slide body) from the formula:

$$y_C[i_0] = \frac{\sum_{j=1}^{N_y} \sum_{k=1}^{N_z} y[i_0, j, k] \cdot m[i_0, j, k]}{\sum_{j=1}^{N_y} \sum_{k=1}^{N_z} m[i_0, j, k]}$$

$$z_C[i_0] = \frac{\sum_{j=1}^{N_y} \sum_{k=1}^{N_z} z[i_0, j, k] \cdot m[i_0, j, k]}{\sum_{j=1}^{N_y} \sum_{k=1}^{N_z} m[i_0, j, k]}$$

10. *Determining an array of points  $C_\varphi[i_0, m]$  in the path  $C(\varphi)$  of the buried part in the conditions of weak rotation of a potential slide body.* Using a mathematical pendulum equation and the coordinates  $C[i_0] = (y_C[i_0], z_C[i_0])$ , we determine the array of points  $C_\varphi[i_0, m] = (y_{C_\varphi}[i_0, m], z_{C_\varphi}[i_0, m])$  ( $m$  is the number of points) describing the path  $C(\varphi)$  at the deviations  $\varphi \in [\varphi_1, \varphi_n]$ :  $C_\varphi[i_0, m] = \cup\{(\sin\varphi, -\cos\varphi)\}$  at  $\varphi = \varphi_1 \dots \varphi_n$  with a pitch  $\pi/180$ , where  $l = \sqrt{(y_T[i_0] - y_C[i_0])^2 + (z_T[i_0] - z_C[i_0])^2}$ . For the limits of the interval  $\varphi \in [\varphi_1, \varphi_n]$ , it is convenient to select  $\varphi_1 = \varphi_0 - \pi/36$  and  $\varphi_n = \varphi_0 + \pi/36$ , which is governed by computational errors in kriging and by small changes in the position of the gravitational center of the buried part at such angles.

11. *In accordance with catastrophe theory, determining a cusp point  $R[i_0]$  for a 2D model  $M[i_0]$ .* From each point  $C_\varphi[i_0, m]$  of the gravitational center path in the buried part, a normal line to a tangent to this point is drawn. The intersection of these normal lines shapes a special geometrical figure called a cusp [15]. The point  $R[i_0] = (y_R[i_0], z_R[i_0])$  with the smallest value along the axis  $Oz$  (out of the values  $z_{C_\varphi}[i_0, m]$ ) is a cusp point. Analytically, this step of the algorithm reduces to derivation of equations for the normal lines to the tangents to the points  $C_\varphi[i_0, m]$ , to pair-wise solving of these equations and finding thereby an intersection point with the least value along the axis  $Oz$ .

12. *Does the cusp point lie below the gravity  $T[i_0]$  or beyond the boundary of a potential body of slide?* If  $z_R[i_0] < z_T[i_0]$  or the point  $(y_R[i_0], z_R[i_0])$  is beyond the boundary of a potential body of slide, go to step 13; otherwise, go the step 14.

13. *The conclusion is: according to the analysis of the section  $i_0$ , the potential body of slide is in the condition of global instability.* Go to step 17.

14. *Do the gravity  $T[i_0]$  and the cusp point lie in the same axis  $Oz$ ?* If  $z_R[i_0] = z_T[i_0]$ , go to step 15; otherwise, go to step 16.

15. *The conclusion is: according to the analysis of the section  $i_0$ , the potential body of slide is in the stable condition.* Go to step 17.

16. *The conclusion is: according to the analysis of the section  $i_0$ , the potential body of slide is in the condition of local instability.* Go to step 17.

17.  $i_0 \leq N_x$ ? If  $i_0 \leq N_x$ , go to step 18; otherwise, go to step 19.



**Fig. 1. Architecture of automated software system**

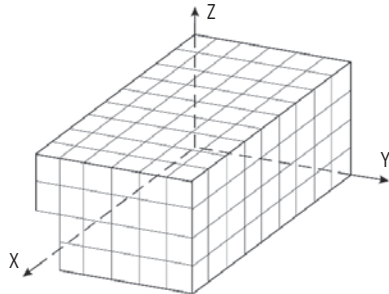


**Fig. 2. Graphic form of reference block model of potential landslide body**

18.  $i_0 \leftarrow i_0 + 1$ . Attribute the value  $i_0 + 1$  to the index  $i_0$ , which points at the discussed 2D block model in the obtained set. Go to step 8.
19. *The end.* Finish the algorithm.

**Results and discussions**

Using the object-oriented design, an architecture of the developed automated software system was built (Fig. 1).

According to this architecture represented using an UML Component Diagram, the system being discussed comprises three subsystems and their interfaces. The first subsystem—*DataAcquisition*—acquires data on moisture, density and displacement of rock mass on the test site of pitwall. The process involves using geodetic equipment, moisture sensors and lab-scale testing of rock density. The second subsystem—*StabilityAnalysis*—uses the captured data to analyze the condition of the test pitwall site to detect local and global instabilities. This subsystem applies the above-described algorithm of the slope stability analysis. The third subsystem—*DataManagement*—is in charge of processing and storage of all sets of data on density, displacement and moisture of rock on the test site. Using the Java language and the Spring Boot framework, the mentioned architecture was implemented as a stand-alone application.

To check the relevance of the decision, the proposed system was tested at the Dzhegonas Quarry in the Karachay–Cherkess Republic, Russia. The geodetic survey detected a potential body of slide in overburden of the upper bench of the pitwall. The overburden represented various genesis sandstones and loams with small pockets of pebble stone. The potential slide body had a length of 10.8 m, width of 7.2 m and a depth of 5 m, which allowed applying the developed automated analysis of a rotational slide potentiality.

Using the data on the boundary of the potential body of slide and the value of the representative volume of rocks ( $V \approx 1.73 \text{ m}^3$ ), the automated software system built an empty 3D model. Then, by setting the found values of displacements, densities of dry rocks and their moisture contents in certain block using the method of kriging, the model was filled with data. The resultant 3D reference block model of the potential

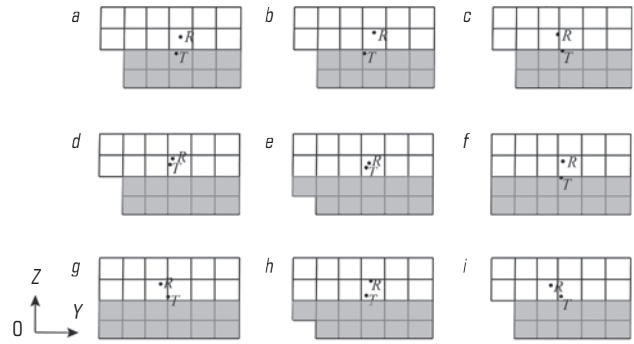


**Fig. 3. Analytical results of 2D block models at:**  
 $i_0 = 1$  (a);  $i_0 = 2$  (b);  $i_0 = 3$  (c);  $i_0 = 4$  (d);  $i_0 = 5$  (e);  $i_0 = 6$  (f);  
 $i_0 = 7$  (g);  $i_0 = 8$  (h);  $i_0 = 9$  (i)



**Fig. 4. Result of rotational landslide on pitwall slope**

body of slide is presented graphically in Fig. 2. The sizes of blocks were assumed to be  $1.2 \times 1.2 \times 1.2 \text{ m}$ .

After analyzing displacements, the system allowed delineating the buried part of the test body. On this basis, the 3D block model of a potential body of slide was obtained with regard to rain precipitations, and then it was split into a set of sections—2D block models.

Each of the models was analyzed to find the values of the governing parameter—the coordinates of the cusp point  $R$  and gravity  $T$  of a section as a whole (Fig. 3). The analysis of the positions of these points revealed a condition reflective of the global instability in the sections with the values  $i_0 = 4$  and  $i_0 = 5$  (see Figs. 3d and 3e). The buried part of the test body is marked with grey color.

Later on, after atmospheric fallout, a rotation landslide was observed on the test site, which resulted in failure of the lower-lying bench (Fig. 4).

**Conclusions**

As a result of the accomplished research, the automated system was designed for the slope stability analysis of pitwall slope areas sensitive to rotational landslide. As against analogous approaches, the proposed system takes into account the actual mechanism of rotational slides, namely, not one but two types of instability of pitwall slopes. In case of the first type—local instability, small displacements of a potential slide body impose no risk on mining operations. In case of the other

type of instability—global instability, the weakest displacements of a potential body of slide can initiate a landslide process. Detection of these instability types became possible owing to a new algorithm of the slope stability analysis for open pit mines. The features of the algorithm are: (1) rigorously formalized physico-mathematical justification of the critical condition analysis of potential slide bodies using catastrophe theory; (2) analysis of a test object as a block model with the formalized delineation method for the buried part of the potential body of slide; (3) inclusion of a governing factor of landslide descent—rain precipitations.

The relevance of the proposed solutions was tested as a case-study of the Dzhegonas Quarry in the Karachay-Cherkess Republic of Russia. According to the test result, the efficiency of the proposed system as percentage of the correct solutions in the stability analysis of pitwall slopes in terms of detected rotational slides was 90%, while software products used at the mine earlier provided only 60% efficiency.

The further research trends may be: (1) improvement of the slope stability analysis for open pits with regard to stress field to enhance delineation accuracy for the buried part of a potential body of slide; (2) application of the proposed algorithm in design of new automated systems for real-time monitoring of pitwall condition.

#### References

1. Bezie G., Chala E. T., Jilo N. Z. et al. Rock slope stability analysis of a limestone quarry in a case study of a National Cement Factory in Eastern Ethiopia. *Scientific Reports*. 2024. Vol. 14, No. 1. ID 18541.
2. Kumar S., Choudhary Sh. Sh., Burman A. Recent advances in 3D slope stability analysis: A detailed review. *Modeling Earth Systems and Environment*. 2023. Vol. 9, No. 2. pp. 1445–1462.
3. Bennouna R., Ouadif L., Akhssas A., Zerradi Y., Bahi A. The application of empirical methods and kinematical analysis to assess the stability of a rock formation—A case study. *Civil Engineering and Architecture*. 2024. Vol. 12, No. 3. pp. 1813–1832.
4. Shariati M., Fereidooni D. Rock slope stability evaluation using kinematic and kinetic methods along the Kamyaran–Marivan road, west of Iran. *Journal of Mountain Science*. 2021. Vol. 18, No. 3. pp. 779–793.
5. Wang Ya., Li Y., Chen J. Comprehensive analysis method of slope stability based on the limit equilibrium and finite element methods and its application. *Open Journal of Civil Engineering*. 2023. Vol. 13, No. 4. pp. 555–571.
6. Alok A., Burman A., Samui P., Kaloop M. R., Eldessouki M. A generalized limit equilibrium-based platform incorporating simplified Bishop, Janbu and Morgenstern–Price methods for soil slope stability problems. *Advances in civil engineering*. *Advances in Civil Engineering*. 2024. Vol. 2024. ID 3053923.
7. Zhu M., Ma C., Tang R. et al. Slope stability analysis of open pit mine based on finite difference method. *2009 Second International Conference on Information and Computing Science*. 2009. pp. 208–211. DOI: 10.1109/ICIC.2009.258
8. Ghedjati S., Lamara M., Houmadi Y. Finite difference probabilistic slope stability analysis based on collocation-based stochastic response surface method (CSRSSM). *Innovative Infrastructure Solutions*. 2020. Vol. 5, No. 3. ID 73.
9. Saim N. M., Kasa A. Comparative analysis of slope stability using Finite Element Method (FEM) and Limit Equilibrium Method (LEM). *2023 IEEE 14th Control and System Graduate Research Colloquium (ICSGRC)*. 2023. pp. 224–229. DOI: 10.1109/ICSGRC57744.2023.10215453
10. Wang Zh., Lin M. Finite element analysis method of slope stability based on fuzzy statistics. *Earth Sciences Research Journal*. 2021. Vol. 25, No. 1. pp. 123–130.
11. Xu GJ., Zhong Kz., Fan Jw., Zhu Ya. J., Zhang Yu. Q. Stability analysis of cohesive soil embankment slope based on discrete element method. *Journal of Central South University*. 2020. Vol. 27, No. 7. pp. 1981–1991.
12. Maleki Javan M. R., Kilanehei F., Mahjoob A. Rock slope stability analysis using discrete element method. *International Journal of Transportation Engineering*. 2015. Vol. 2, No. 3. pp. 199–211.
13. Liu P, Rui Yi, Wang Yu. Study of the sliding friction coefficient of different-size elements in discrete element method based on an experimental method. *Applied Sciences*. 2024. Vol. 14, No. 19. ID 8802.
14. Khalkechev R. K. About one new scheme for the application of finite element method in mining sciences. *Sustainable Development of Mountain Territories*. 2024. Vol. 16, No. 2(60). pp. 612–619.
15. Khalkechev K. V., Khalkechev R. K. Application of catastrophe theory for mathematical modeling of landslide process on concave slopes of mountain territories. *Sustainable Development of Mountain Territories*. 2023. Vol. 15, No. 3(57). pp. 720–726.
16. Sim K. B., Lee M. L., Wong S. Y. A review of landslide acceptable risk and tolerable risk. *Geoenvironmental Disasters*. 2022. Vol. 9, No. 1. ID 3.
17. Khalkechev K. V., Khalkechev R. K. Mathematical model development of a surface translational landslide with a sod on straight slopes of mountain territories during atmospheric precipitation. *Sustainable Development of Mountain Territories*. 2024. Vol. 16, No. 1(59). pp. 174–180.
18. Knuth D. E. *The Art of Computer Programming*. Vol. 1: Fundamental Algorithms. Boston : Addison-Wesley, 1997. 655 p.
19. Khalkechev R. K. Stochastic determination of unit volumes in crystal and composite geomaterials. *News of the Kabardino-Balkarian Scientific Center of RAS*. 2012. No. 2-2 (46). pp. 38–41.
20. Baikov V., Bakirov N., Yakovlev A. *Mathematical Geology*. Izhevsk : Institute computernikh issledovaniy, 2012. Vol. I. 228 p. 